Source and biological response of biochar organic compounds released into water. Relationships with bio-oil composition and carbonization degree

Source and biological response of biochar organic compounds released into water. Relationships with bio-oil composition and carbonization degree

Michele Ghidotti,[*,†,¶] *Daniele Fabbri,*[†,¶] *Ondřej Mašek,*[‡] *Colin Logan Mackay,*[§] *Marco Montalti,*[¶] *Andreas Hornung,*[⊥]

[†]Interdepartmental Centre for Industrial Research "Energy and Environment" and Department of Chemistry "Giacomo Ciamician", University of Bologna, via S. Alberto 163, I-48123 Ravenna, Italy, michele.ghidotti2@unibo.it, +39 0544 937388; [‡] UK Biochar Research Centre, School of GeoSciences, University of Edinburgh, Crew Building, Alexander Crum Brown Road, Edinburgh, United Kingdom; § SIRCAMS, School of Chemistry, University of Edinburgh, Joseph Black Building, King's Buildings, West Mains Road, Edinburgh, United Kingdom; [¶]Department of Chemistry "G. Ciamician", University of Bologna, Via Selmi 2, Bologna, Italy; [⊥]Fraunhofer Institute for Environmental, Safety, and Energy Technology UMSICHT, Institute Branch Sulzbach-Rosenberg, An der Maxhütte 1, 92237 Sulzbach-Rosenberg, Germany

ABSTRACT

Water-soluble organic compounds (WSOCs) were extracted from corn stalk biochar produced at increasing pyrolysis temperatures (350-650°C) and from the corresponding vapors, collected as bio-oil. WSOCs were characterized by gas chromatography (semi-volatile fraction), negative

electron spray ionization high resolution mass spectrometry (hydrophilic fraction) and fluorescence spectroscopy. The pattern of semi-volatile WSOCs in bio-oil was dominated by aromatic products from lignocellulose, while in biochar was featured by saturated carboxylic acids from hemi/cellulose and lipids with concentrations decreased with decreasing H/C ratios. Hydrophilic species in poorly carbonized biochar resembled those in bio-oil, but the increasing charring intensity caused a marked reduction in the molecular complexity and degree of aromaticity. Differences in the fluorescence spectra were attributed to the predominance of fulvic acid-like structures in biochar and lignin-like moieties in bio-oil. The divergence between pyrolysis vapors and biochar in the distribution of WSOCs with increasing carbonization was explained by the hydrophobic carbonaceous matrix acting like a filter favoring the release into water of carboxylic and fulvic acid-like components. The formation of these structures was confirmed in biochar produced by pilot plant pyrolysis units. Biochar affected differently shoot and root length of cress seedlings in germination tests highlighting its complex role on plant growth.

INTRODUCTION

Biochar (BC) research has made consistent progress since it was proposed as a sustainable strategy for the abatement of greenhouse gases in terrestrial ecosystems.[1] However, the ameliorating effect of BC in soil applications is highly dependent on its physical and chemical properties, in turn affected by production technology and biomass feedstocks. The definition of BC quality is therefore fundamental, and different criteria were proposed for its classification, like carbon content, aromaticity, and the presence of harmful chemical species such as heavy metals or polyaromatic hydrocarbons (PAHs).[2] Apart from priority contaminants, the role of BC mobile organic compounds is being evaluated as potentially affecting its performance in soil. Volatile

organic compounds (VOCs) and water soluble organic compounds (WSOCs) were deemed responsible for the positive[3] and negative[4,5] effects on plants, microorganisms[6] and aquatic organisms[7,8]. BC labile carbon structures could also affect the composition of soil derived dissolved organic matter, in turn influencing soil ecosystem processes. The presence of organic species leached from BC was confirmed in soil application. Riedel et al.[9] evidenced a compositional change in the molecular fingerprint of the organic matter released from a soil mixed with BC compared to untreated soil in column experiments. The amendment caused a marked reduction of the organic matter mobilization from the soil, but a net increase in the intensities of black carbon-type and lignin-type compounds was observed. Uchimiya et al.[10] demonstrated the existence of polyaromatic moieties in the dissolved organic carbon (DOC) extracted from a BC-amended soil, attributed to unique structures of pyrogenic DOC. Vapors re-condensation and pyrolysis temperature were found to be of primary importance for the production of BC suitable for soil application[5,8,11]. The contact of the pyrolysis vapors with the carbonized biomass inside the reactor and their removal is critical to prevent BC contamination[5,8]. Temperature and residence time are crucial process parameters. At temperatures higher than 400°C a sharp decrease in VOCs adsorbed on BC was evidenced[8,11]. High nitrogen flow can reduce the content of PAHs[12,13]. The effect of process conditions on the composition of WSOCs has not been widely investigated, nonetheless WSOCs may play an important role in BC environmental impact due to their mobility in water. WSOCs were investigated by means of two dimensional GC[8] and liquid chromatography[3,14,15], while ultrahigh resolution mass spectrometry (Fourier Transform Ion Cyclotron Resonance Mass Spectrometry FT-ICR-MS) revealed the presence of thousands hydrophilic species, non-detectable with other techniques [8,9,16]. Fluorescence spectroscopy with Parallel Factor Analysis (PARAFAC) was used as rapid and sensitive technique to investigate its

aromatic fraction[10,17–19]. These studies have noticeably increased our understanding on the chemical composition of BC WSOCs, however, the relationship with production parameters and especially with the composition of the pyrolysis vapors are poorly known. The present study was primary focused on the comprehensive characterization of BC WSOCs with spectroscopic, chromatographic and mass spectrometry techniques in relation to the composition of the water-soluble fraction of the pyrolysis vapors, condensed (bio-oils) during the pyrolyses for BC production. The linkage between WSOC patterns, BC bulk properties and their implications on seeds germination, could eventually shed light on the role of BC mobile organic compounds in the determination of its quality for environmental applications, possibly leading to the proposal of threshold levels.

MATERIALS AND METHODS

Samples

BC were produced from pelletized corn stalks at 350, 400, 450, 500, 550, 600, 650°C and characterized in a previous study.[11] The vapors carried by the nitrogen flow at the outlet of the reactor presented temperatures ranging from 195°C (pyrolysis at 350°) to 310°C (pyrolysis at 650°C), measured with a thermocouple. These values were considered sufficiently high to minimize vapors re-condensation in the part of the reactor where the biochar was synthesized. Vapors leaving the reactor were condensed in two ice/salt cold traps at -14°C to collect the pyrolysis liquids. The content of the two traps was merged to produce one bio-oil (OL) sample per temperature. In this study, the samples produced at the temperature *XXX* °C are named *BCXXX* and *OLXXX*.

Lipid extraction from corn stalk biomass

87 The total lipid fraction of the corn stalk biomass used in the pyrolysis experiments was determined
88 by sequentially extracting the feedstock with $CHCl_3$-MeOH 2:1 (v/v) at 50°C for 1.5 hours
89 (triplicate analysis). The profile of fatty acids was determined by GC-MS after methanolysis
90 followed by the production of fatty acid methyl esters (FAME)[20].

91 *Extraction of biochar WSOCs*

92 An amount of BC was weighed (1 g ± 0.01 mg) into 20 ml vials and 10 ml of deionized water
93 (DW, HPLC grade) was added. The vials were sealed with aluminum crimp seals with
94 PTFE/rubber septa. The sealed vials were then placed on a mechanical shaker (IKA KS 260)
95 covered with an aluminum foil, and left shaking at 150 rpm for 72 hours at ambient temperature.
96 The resulting solutions were centrifuged at 3800 rpm for 10 min (ALC4232 centrifuge) to separate
97 the solid material and filtered with PTFE syringe filters 0.45µm (Sartorius Minisart SRP)
98 thereafter.

99 *Analysis of BC WSOCs by direct immersion (DI)-SPME-GC-MS*

100 Each BC extract (1ml) was added with 0.5 ml of 2M phosphate buffer (KH_2PO_4/Na_2HPO_4) at pH
101 5.7 in 1.5 ml vials. Carboxen-PDMS (Car-PDMS) SPME fiber was exposed to the solution under
102 magnetic stirring for 30 minutes.[4] The thermal desorption of the analytes and GC-MS analysis
103 were performed with the method developed in a previous study[11]. The amounts of WSOCs were
104 expressed as peak area counts normalized by the sample weight (*NA*). Blank analyses of phosphate
105 buffer and DW were performed to check procedural contaminations. A calibration curve of volatile
106 fatty acids (VFA) was performed with a standard VFA solution (0.1% Sigma-Aldrich) containing
107 acetic acid, propanoic acid, methyl propanoic acid, butanoic acid, 3-methyl butanoic acid and
108 pentanoic acid in DW. Serial dilutions were prepared at 10, 5, 1 and 0.1 mg/l in phosphate buffer,

spiked with 2-ethyl butyric acid 5mg/l in DW (internal standard) and analyzed in triplicate. The concentration of each VFA was calculated using the response factors from the calibration curve and expressed as ($\mu g/g_{BC}$).

Analysis of BC WSOCs by ESI(-)FT-ICR-MS

BC extracts were diluted 1:10 in methanol and analyzed by negative electrospray ionization (capillary voltage 4kV) on a Bruker solariX 12T FT-ICR-MS. 500 scans were acquired for each spectrum (syringe infusion, $200\mu L \cdot h^{-1}$) using an 8 MW acquisition size (broadband). Ion accumulation time was set at 0.8sec. Samples were spiked with ES tuning mix (Agilent) and a starting calibration list was developed from single point correction on the m/z 301.998139. Mass spectra were analyzed using Data Analysis software (Bruker Daltonics). Peaks were assigned with a signal to noise threshold of 4 and absolute intensity threshold of $2 \cdot 10^6$. Calibration lists were developed over the m/z range 100-600 by Kendrick mass analysis. Mass spectra without the calibrant were recalibrated with a quadratic equation with a standard deviation < 100ppb (67 points). Calibrated mass lists were processed with PetroOrg software. Peaks were assigned with a threshold of 100ppb and molecular formulas within the range: $C_{1\text{-}100}$, $H_{4\text{-}200}$, $O_{1\text{-}20}$, $N_{0\text{-}4}$.

Analysis of BC WSOCs by fluorescence spectroscopy and PARAFAC

BC extracts were diluted in DW until the absorbance in the UV-Vis wavelength range 200-800 nm was <0.1[21], recorded with a PerkinElmer λ650 spectrophotometer, using quartz cells with 1.0 cm optical path. Fluorescence excitation/emission matrices (EEMs) were acquired (duplicate analysis) on an Edinburgh Instrument F900 with excitation and emission wavelengths in the range of 220-500 and 280-600 nm respectively, both at 5nm intervals. Solutions of 16 EPA PAHs (Sigma-Aldrich, 1μg/ml), IHSS Suwanee River Fulvic Acid (SRFA, 1mg/ml), *o*-cresol and *o*-eugenol (0.1

131 mg/ml) in DW were analyzed under the same conditions. PARAFAC was performed on the EEMs
132 corrected for instrument bias and non-trilinear signals, with N-way toolbox[22], drEEM tool for
133 Matlab [23].The number of PARAFAC components was selected considering the Stoke's shift,
134 leverage values, analysis of residuals and core consistency diagnostic[23,24].

135 *Analysis of bio-oil WSOCs*

136 The OL samples were diluted 1:10 in DW and centrifuged (3800 rpm for 15 min) to precipitate
137 the water-insoluble part, while the WSOCs were analyzed by DI-SPME-GC-MS, FT-ICR-MS and
138 fluorescence-PARAFAC. An aliquot of 250µl was spiked with 150 µl of *o*-eugenol 10 µg/ml in
139 DW, phosphate buffer and DW to a final volume of 1.5 ml. DI-SPME and GC-MS conditions were
140 those used for BC. FT-ICR-MS was performed on solutions further diluted 1:100 in methanol. 500
141 scans were acquired for each spectrum using an 8 MW acquisition size (broadband). Ion
142 accumulation time was set at 0.5sec. Peaks were assigned with a signal to noise threshold of 4 and
143 absolute intensity threshold of $2 \cdot 10^6$. Mass spectra without the calibrant were recalibrated with a
144 quadratic equation with a standard deviation < 100ppb (89 points). Calibrated mass lists were
145 processed with PetroOrg software. Peaks were assigned with a threshold of 100ppb and molecular
146 formulas within the range: $C_{1\text{-}100}$, $H_{4\text{-}200}$, $O_{1\text{-}20}$, $N_{0\text{-}4}$, $S_{0\text{-}2}$. Fluorescence-PARAFAC conditions were
147 the same used for BC.

148 *Germination tests*

149 Seed germination tests on cress (*Lepidium sativum L.*) were conducted with BC in water
150 suspensions at 40g/l (4 replicates) according to Rombolà et al.[4]. A solution of acetic, propanoic,
151 butanoic and 3-methyl butanoic acid in DW (98, 18, 7.6, 1.4 mg/l respectively) was also tested,
152 alone and with BC650 at 40g/l. Fifteen seeds per Petri dish were sampled and seedlings elongation
153 was measured (root and shoot lengths in cm). The following statistics were performed with the

154 software PAST (Paleontological Statistic vers. 2.16): Kruskal-Wallis test (non-parametric), one-
155 way ANOVA (after data transformation with Box-Cox, to achieve normality of the distributions
156 and homogeneity of the variance), post-hoc tests (Mann-Whitney and Tukey test)

157 *WSOCs of biochar from pilot plant pyrolysis units*

158 A set of five BC samples produced with pilot plant pyrolysis units were extracted with DW and
159 WSOCs characterized by DI-SPME and Fluorescence-PARAFAC. Two reference BC from
160 miscanthus straw (MSP550) and softwood pellets (SWP550) produced at 550°C with a 50 kg/h
161 capacity unit were purchased from the UK Biochar Research Centre, University of Edinburgh.
162 Three BC samples produced with PYREG and characterized in an interlaboratory ring trial (EU-
163 COST Action TD1107)[2] were also investigated. These samples were produced from residues of
164 wood chips production (BC1), a blend of paper sludge and wheat husks (BC2), and sewage sludge
165 (BC3) at 620, 500 and 600°C respectively.[2]

166 **RESULTS AND DISCUSSION**

167 *Semi-volatile WSOCs (DI-SPME-GC-MS)*

168 The corn stalk BC and the corresponding OL presented noticeable dissimilarities in the patterns of
169 semi-volatile WSOCs. Representative examples are reported in the chromatograms of Figure 1,
170 while all the compounds detected in BC and OL are listed in Table S1 and S2 respectively. The
171 series of peaks in BC350 extracts were predominantly associated to carboxylic acids, which were
172 the main components of the low molecular weight fraction of BC WSOCs, with C_{1-12} straight-
173 chain and branched, saturated and unsaturated aliphatic acids, and aromatic acids like benzoic acid
174 and its C_{1-2} alkylated derivatives. The composition of the OL was more complex (Figure1), with
175 124 tentatively identified compounds in contrast with the 36 of BC350. OL profiles included
176 primarily lignin markers (2-methoxy-, 2,6-dimethoxy- and C_{1-3} alkyl substituted phenols) and

177 typical degradation products of the cellulose and hemicellulose fractions of the parent corn stalk
178 (5-6 membered rings heterocyclic aldehydes ketones and diketones, C_{1-3} alkyl substituted and
179 hydroxyl substituted cyclopentenones, and furans). Only 5 lignin markers characterized BC
180 WSOCs out of the 15 of OL (phenol, C_{1-2} phenols, guaiacol and 4-methyl guaiacol). Their signals
181 became negligible in the BC produced above 500°C. However, traces of alkylated phenols were
182 observed in all the BC WSOCs, possibly indicating their stronger interaction with the aromatic
183 structure of the BC compared to the methoxylated homologues. Furthermore, WSOCs of BC
184 produced below 450°C featured 8 proxies of hemicellulose (furfural and methyl furfural,
185 benzaldehyde and hydroxyl benzaldehyde, 2-acetyl furan and C_{1-3} cyclopentenones) compared to
186 the 34 of OL. A series of compounds generated by the progressive carbonization of the biomass
187 inside the reactor during the pyrolysis were detected in all the OL, like monoaromatic
188 hydrocarbons (benzene, toluene and C_{1-5} alkylated derivatives), and low molecular weight PAHs.
189 None of these species characterized the BC WSOCs, but minor contribution of some of these
190 compounds was evidenced in other studies[8]. Low molecular weight aliphatic aldehydes (C_{3-4}),
191 ketones and diketones (C_{4-6}) were detected in the OL, but not in BC WSOCs, indicating that, if
192 retained by the BC after their production, they could be released preferentially as VOCs.[11] OL
193 composition included also nitrogen containing aromatic compounds deriving from the protein
194 fraction of the biomass feedstock (pyridines, pyrazines, aromatic nitriles quinolines and indoles).
195 Interestingly, BC WSOCs did not present any of these species, indicating an effective removal as
196 pyrolysis vapors or a stronger interaction with BC. Finally, VFA, C_{3-5} unsaturated and higher
197 molecular weight aromatic acids were present in the OL as free carboxylic acids but also in the
198 form of methyl esters, probably originated from the reactivity with methylating products (e.g.
199 methanol) at low pH. OL WSOCs lacked in the C_{4-12} and the methyl substituted homologues of

carboxylic acids, indicating their possible formation and preferential adsorption onto the BC surface during pyrolysis. However, it cannot be excluded that the mass spectra of the missing aliphatic acids, were covered by the dominance of other more intense signals from lignin. The formation of low molecular weight fatty acids during pyrolysis (acetic and propanoic) is associated with the thermal decomposition of the hemi/cellulose fraction. Nevertheless, the higher molecular weight fatty acids could form from the fragmentation of the parent corn stalk lipid fraction. The lipids accounted for 7.0 ± 0.7 % of the biomass dry weight. The pattern of FAME by GC-MS revealed a total of 14 compounds (Table S3), ranging from saturated (8:0-30:0) to unsaturated species (16:1, 18:1 and 18:2). Palmitic, stearic, linoleic and oleic acids were the principal constituents of the FAME in corn seeds,[25] whose residues left in the field could contribute to the composition of the collected corn stalk. A net decrease of the fatty acids was observed in the WSOCs of BC with increasing carbonization degree, measured by the H/C atomic molar ratio. Trace amounts were released even by highly carbonized BC (H/C 0.32), while branched and $C_{3\text{-}7}$ unsaturated homologues were typical of less carbonized ones (H/C 0.80-0.59). In accordance with their presence in the water extracts, fatty acids were also volatilized by BC in the form of methyl esters [11]. Rombolà et al.[4] evidenced the inhibiting activity of WSOCs of poultry litter BC on the germination of cress and VFA were the potential cause. Due to their mobility in air and solubility in water, VFA could play a considerable role in the agronomic/environmental performance of BC application to soil and their quantification could be useful for the determination of its quality. Total VFA concentrations decreased with the increasing BC production temperature from 3.0 ± 0.3 mg/g of CS350 to 35 ± 14 µg/g of CS650 and statistically significant correlations (r> 0.9, p<0.01) were observed between the values of each single and total VFA (Figure S1/TableS4) and the decreasing H/C values of the BC. This correlation is in line with the decreasing amount of VOCs[11]. In

summary, the great majority of species detected in the OL WSOCs were not found in the water extracts of BC. While OL WSOCs featured mostly lignocellulosic derived pyrolysis products, BC was dominated by carboxylic acids from hemi/cellulose and lipids.

Hydrophilic WSOCs (ESI-FT-ICR-MS)

BC contamination could occur if pyrolysis vapors are not correctly swept from the reactor during its production.[5,8] Given the divergent patterns of BC and OL WSOCs discussed in the previous section, the comparison was extended to the less-volatile components that could be detected by ESI(-)FT-ICR-MS. Because ionization with ESI is suitable for polar compounds with both acidic and basic functionalities,[26] the fraction investigated was categorized as hydrophilic. The mass spectra of the OL WSOCs confirmed the complex composition evidenced in other studies on similar feedstocks,[27] as molecular formula assignment allowed to identify up to 4000 peaks (Table S5 and S6). Oxygenated ($C_cH_hO_x$) and nitrogen ($C_cH_hN_yO_x$) species together accounted for more than 60% of the total intensity. Trace contribution of sulfur was observed. The $C_cH_hO_x$ distributions were similar in all the OL, encompassing oxygen atoms in the range $O_{1\text{-}16}$, with O_5 and O_6 as most abundant classes (Figure S2). Interestingly, the N_1O_x class, followed the same pattern with NO_6 as most abundant group, while for the minor N_2O_x and N_3O_x classes, O_4 and O_3 species had the highest abundance (Figure S3). The number of identifiable peaks in the WSOCs of BC350 and BC400 was comparable to that of the OL (about 2000) but sharply decreased to 40 in BC650 (Table S7 and S8). In contrast to the dissimilarities evidenced in the GC detectable fraction, the distribution of WSOCs in BC and OL pictured by ESI presented common features, with $C_cH_hO_x$ compounds as most abundant, followed by the $C_cH_hN_yO_x$ distributions (Table S5 and S7). The same range of oxygen atoms characterized BC350 and BC400 with O_5 as most abundant group, but from BC450 the distributions progressively shifted to the prevalence of O_2 species

(Figure S2). The oxygenated species of BC WSOCs revealed a high bioactivity, as some carboxyl and hydroxyl functionalities were the main source of toxicity on algal growth.[7,16] Given their prevalence in both the BC WSOCs and the OL, the attention was focused primarily on $C_cH_hO_x$ compounds. Van Krevelen diagrams are useful to understand the nature of these species as the molecular formula assigned in the mass spectra can be compared to the major biochemical classes of compounds [28]. To highlight the considerable changes occurring in the WSOCs of OL and BC due to the pyrolysis temperature, Van Krevelen plots of the samples produced at 350, 450, 650°C are reported in Figure 2. The patterns of OL350, 450 and 650, suggest that the pyrolysis temperature did not affect OL composition. Contrarily, those of BC450 and BC650 were distinctly different compared to the corresponding OL, and the increasing BC production temperature caused a net decrease in the number of WSOCs. However, BC350 and OL350 were highly similar, with the series of O_x classes shifting towards higher values of O/C, as consequence to the increasing number of oxygen atoms. Linear regression of the data points in Figure 2 revealed two main pathways: series with an intercept of 2 and those aligning along the equation y=2x. The first one is associated to species differing by units of CH_2[28]. Coherently, alkyl chain elongation was observed also in all the principal compound classes of the volatile and semi-volatile fractions of BC and OL WSOCs (organic acids class, aldehydes, ketones, phenols and mono-aromatic hydrocarbons), as evidenced in Figure S4, where Van Krevelen plots of BC350 and OL350 mass spectra by GC-MS were produced. The latter pathway is indicative of dehydration reactions. Noteworthily, BC350, BC400 and all the OL displayed a point with coordinates (1,2) and molecular formula $C_6H_{12}O_6$, that could be tentatively attributed to glucose or one of its isomers. The dehydration pathway could play an important role in the formation of BC and OL WSOCs from the pyrolysis products of the cellulose/ hemicellulose, as many data points in Figure 2 fall in

269 the region conservatively attributed to carbohydrates (0.67<O:C<1.2, 1.5<H:C<2.4)[29]. Differently,
270 Kendrick mass defect analysis, revealed chain elongation of molecular formulas ascribed to
271 guaiacols and syringols, which were confirmed by DI-SPME analysis. Therefore, the O_2 and O_3
272 species appearing in the region attributed to lignin structures 0.1<O:C<0.7, 0.7<H:C<1.5[30], could
273 be assigned to higher molecular weight phenolic functionalities originated from the pyrolysis of
274 the corn stalk lignin fraction. Similarly, those with higher oxygen content within the same range
275 of H:C and O:C values could represent dimers, trimers or higher molecular weight homologues.
276 Their presence in the BC WSOCs could led to the release of lighter monomers in water by
277 photochemical degradation[31]. Several peaks fell in the region indicative of lipids (1.6<H:C<2,
278 0<O:C<0.2 [28]), and especially the O_2 species can be correlated to analogues of the fatty acids
279 composing the lower molecular weight WSOCs. Generally, the carbon numbers of all the OL
280 WSOCs were comparable to that observed by Hertzog et al in the OL of a lignocellulosic material
281 [32]. Likewise, the values ranged from 5 to 35 in BC350 and BC400 (Figure 3), corroborating the
282 similarity between the WSOCs of poorly carbonized BC and those of OL. Double bond equivalent
283 (DBE), or degree of unsaturation is the number of rings and double bonds and can provide
284 information on the aromaticity of the WSOC species. The DBE values ranged from 1 to 18 in
285 BC350, BC400 and all the OL. For DBE>2 an increase in the carbon number was associated to an
286 increase of the number of oxygens (Figure 3). In summary, BC350 and BC400 WSOCs resembled
287 those of the OL, but for BC>450 the cellulose and hemi-cellulose derivatives disappeared (Figure
288 2 and S4), while lignin degradation products could be detected until 550°C (BC550). The trend
289 was associated to a sharp decrease of the more aromatic species with DBE>10 (Figure 3). At higher
290 pyrolysis temperatures (> BC550), WSOCs tended to have increased H:C and low DBE values

291 (<5) ascribable to organic acids, still detectable at the highest pyrolysis temperature (BC650)
292 (Figures 2 and 3).

293 *Aromatic structures of biochar WSOCs (Fluorescence-PARAFAC)*

294 All the aqueous extracts of BC and OL exhibited fluorescence indicative of the occurrence of
295 aromatic functionalities. Figure S5 reports the EEMs of the BC and OL WSOCs, and those of the
296 standard compounds, that were acquired to qualitatively compare known chemical species with
297 the aromatic structures recurring in biochar WSOCs. PAHs were selected for their high
298 fluorescence even though detected only in traces in the chromatograms of the OL (Table S2),
299 alkylated and methoxylated phenols (*o*-cresol and *o*-eugenol) as lignin derivatives, and IHSS-
300 SRFA as model humic substance. A PARAFAC model with 4 components (C1-4) suitably
301 represented the dataset (95% of the variance explained) and is reported in Figure 4. C1 and C2
302 presented excitation/emission maxima at 320/405 and 350/470 nm respectively. Fluorophores of
303 the natural organic matter (NOM) are characterized by broad excitation/emission spectra, with
304 representative peaks in the wavelength range of 300-370/400-500 nm.[33] Zhongqui et al.[34]
305 characterized 13 IHSS standard humic substances (aquatic and soil derived humic and fulvic acids)
306 with PARAFAC, and two components resembled C1 and C2, while the spectral characteristics of
307 IHSS-SRFA in Mobed et al.[35] showed the same peaks at 320/405 and 350/470. C3 and C4 featured
308 maxima at 285/335 and 275/310 nm respectively. Similar peaks in NOM were associated to
309 protein-like structures.[33] The intensities of the PARAFAC components are reported in Table S9,
310 and their relative percent contributions to the total signal of each sample are presented in Figure
311 S6. The BC WSOCs were mainly composed by C1 and C2 and lacked in the C3 and C4 structures,
312 that featured the OL. Overall, the total signal intensity of BC WSOCs sharply decreased from
313 BC450 and likewise that of C1 and C2, even though were still detectable at 650°C (Table S9).

Contrarily, the total EEM intensity of the OL was not dependent on the pyrolysis temperature and showed values one order of magnitude higher than that of the BC (Table S9). The percent contribution of C1 sharply increased with the pyrolysis temperature in the BC WSOCs while C2 decreased accordingly. Similar trends were observed by Uchimiya et al.[19] in which pyrogenic DOC of lignocellulosic and animal based BC were investigated: two peaks (310/420 and 350/470 nm) were attributed to polyphenolic pyrolysis products and aromatic humic-like compounds that decomposes above 350°C, with the first one increasing and the second one decreasing with the pyrolysis temperature. C3 presented a maximum in OL350 and decreased at higher temperatures, while C4 smoothly increased. A high contribution of C3-C4-like components was observed in non-completely pyrolyzed BC from sawmill waste feedstocks[18] and the pyrolysis of lignocellulosic biomass with low nitrogen and sulfur content is known to produce phenolic species. Given the low nitrogen content in the BC (1%)[11], and their similarity with the EEMs of the lignin markers (Figure S5), C3 and C4 could be associated to phenolic-like species. However, it cannot be excluded that protein-like structures could contribute to C3, as several nitrogen-containing compounds were detected in the OL. Moreover, the standard PAHs solution showed a similar peak at 280/335 nm, that could be attributed the naphthalene or fluorene[36]. Nevertheless, PAHs exhibited distinctively narrower peaks compared to the broader ones observed for C1 and C2. Noteworthily, C3 and C4 had lower emission wavelengths than C1 and C2. A red shift in the excitation/emission maximum can be associated to an increased aromaticity and higher molecular weight,[17,18] therefore C3 and C4 presented a lower degree of aromaticity compared to C1 and C2. Similarly, Uchimiya et al.[17] observed a component comparable to C2 (380/460 nm) that was associated to recalcitrant polyaromatic fraction substituted with carboxyl and phenolic functionalities, especially in low temperature BC (350-500°C). In summary, BC WSOCs were composed of fulvic-like structures

and depleted in the phenolic-like less aromatic functionalities C3 and C4. Interestingly C1 and C2 were also primary components of the OL suggesting that biomass pyrolysis could intrinsically produce aromatic NOM-like moieties.

Effects on the germination of cress seeds

Germination tests are simple bioassays to screen the potential phytotoxicity of BC in soil due to the presence of harmful compounds (metals, PAHs, carboxylic acids, phenols).[4,5,37] Tests on cress seeds aimed to evaluate the performance of BC containing variable amounts of WSOCs in consequence to the pyrolysis temperature. The ratio BC/DW of 40 g/l was chosen as indicative of a relatively high load of BC in soil application (40 t/ha). Lower loads were considered less active,[3] while higher values less realistics,[10,38] and were not examined in this study. The germination rate with BC was not significantly different from the controls without BC ($p > 0.05$) and the average value of all the treatments was 97 ± 2.5 %. In agreement with previous studies on corn stalk BC with high VOC content,[11] WSOCs did not present inhibiting effect. Surprisingly, the seedlings emerged after the germination showed significantly longer shoots in all the BC treatments versus the controls ($p < 0.001$), and the values for the BC with greater WSOCs content (BC 350-500) were higher ($p < 0.05$) than those of the more carbonized ones (BC 550-650) (Figure 5). BC WSOCs could be involved in the enhancement of plant growth. Plant stimulants such as karrikins[39] were recently detected in green waste BC and in the corresponding pyrolysis water, particularly KAR1 (3-methyl-2*H*furo[2,3-*c*]pyran-2-one), that induced longer shoot lengths of tomato and lettuce seedlings in germination tests.[40] Interestingly, ESI(-)FT-ICR-MS mass spectrum of all the OL presented a peak at *m/z* 149.02442 $[M-H]^-$ with molecular formula $[C_8H_5O_3]^-$, that could be associated to KAR1. However, the peak was not revealed in corn stalk BC WSOCs, probably because of the trace concentration reported in BC compared to pyrolysis water[40]. Moreover, BC

WSOCs featured aromatic fulvic-like structures and humic substances were found to promote the growth of shoot and roots of plants at different stages.[41] With regards to the semi-volatile fraction, a solution of VFA mimicking the concentrations detected in BC350 (3 mg/g_{BC}) was tested without and with BC650 (this BC was almost deprived of VFA Table S4). Total VFA concentration of 125 mg/l (equivalent to 40 g/l load of biochar) exhibited the same effects of the control in the case of the solution with only VFA, and the same effect of BC650, when added to the corresponding biochar (Figure 5). These findings indicated that VFAs were not involved in the root and shoot growth. Contrary to the improved shoot growth, significantly shorter root lengths were observed in the BC versus the controls ($p < 0.001$), especially BC550-650 ($p < 0.001$) (Figure 5). Reduced root growth was observed by Buss et al.,[38] who associated the inhibition to high pH and available K of biochar produced in the temperature range of 550-650°C. However, the same study reported also the inhibition of shoot growth.[38] Lengthening of root in plants is connected to the exploration of soil for water and nutrients during drought periods.[42] In Petri dish bioassays, where the water content is not a limiting factor and the nutrients are provided by the seeds, BC could have possibly promoted the investment of carbon in the shoots rather than the roots. This would explain the improved shoot and reduced radical length for all BC. A similar effect was observed also on maize seedlings with maize BC produced at 450°C.[43] However, the inhibition of root growth due to inorganic components or pH, cannot be excluded, and other factors could contribute to the improved shoot lengths, like the provision of additional nutrients by the BC.

Implications for biochar environmental applications

In this study, it was shown that after three days in water at r.t, even highly carbonized BC released WSOCs. Interestingly, in a leaching study lasted for 17 days, most of the BC WSOCs were released within the first 3 days of the experiment.[18] Thus, under environmental conditions, a wide

383 array of compounds can contribute to the pool of natural organic matter in soil. Overall, SPME-
384 GC-MS, ESI(-)FT-ICR-MS and fluorescence-PARAFAC indicated that the release of WSOCs
385 from BC was strongly reduced above 450°C, in agreement with the trend observed for VOCs, that
386 began to decrease above 400°C.[11] The investigation of OL WSOCs revealed original clues about
387 the formation and release of those from BC. Organic acids were the main semi-volatile components
388 released in water, suggesting that the more abundant OL components of lignin were strongly
389 adsorbed onto the BC matrix or efficiently volatilized during pyrolysis. Given the porous structure
390 of biochar, pores could be accessible by water solutions and the retention of phenolic compounds
391 could possibly occur due to a hydrophobic effect, or by π-π interactions,[44] that become more
392 pronounced as the matrix gets more carbonized[45]. Previous studies categorized biochar water-
393 extractable organic compounds into classes used to describe NOM and evidenced that low
394 molecular weight acids were important species even in BC produced at higher temperatures, while
395 humic acids and low molecular weight neutral species were the principal components of the lower
396 temperature BC (<450°C)[14,46]. The higher molecular weight and aromatic structures of BC
397 WSOCs were comparable to the species recurring in NOM. In D'Andrilli et al.[33] the standard
398 IHSS-SRFA was dominated by $C_cH_hO_x$ species by ESI(-)FT-ICR-MS and likewise BC and OL
399 WSOCs of this study, that displayed similar structures in the lignin region of the Van Krevelen
400 diagrams, but unique formulas in that of carbohydrates and lipids. Besides, the principal mass
401 spacing patterns in the mass spectra (ESI-FT-ICR-MS) were alkyl chain elongation (14.01565 Da)
402 and substitution of CH_4 versus O (0.0364 Da)[47] in both SRFA and WSOCs. Fluorescence EEMs
403 further confirmed the fulvic-like nature of the BC WSOCs, that was composed of labile (C1) less
404 aromatic, and more recalcitrant polyaromatic (C2) structures substituted with carboxyl and
405 hydroxyl groups, in agreement with previous hypotheses.[10,17,48] WSOCs were extracted from five

406 BC produced by pilot plant continuous pyrolysis units. The profiles of semi-volatile and aromatic
407 WSOCs are reported in Figure S7 and S8, respectively. BC1, 2 and 3 did not present detectable
408 peaks associated to semi-volatile species. These BC were stored outdoors for several days after
409 production and the more volatile components, if present, could have been lost. MSP550 and
410 SWP550 BC, sealed upon production to prevent contamination, presented trace intensities of acetic
411 acid, in line with the carboxylic acids released in water by corn stalk BC produced at the same
412 temperature (BC550). However, the patterns of semi-volatile WSOCs were markedly reduced
413 compared to BC550 (Figure S7), indicating that some vapor re-condensation could have occurred
414 in the bench scale reactor. Interestingly, the EEMs of the WSOCs extracted from all the
415 commercial BC revealed fluorophores resembling the aromatic fulvic-like structures C1 and C2
416 (Figure S8). This finding suggests that even at the pilot plant scale these aromatic units are formed
417 probably by the interaction between the pyrolysis vapors and BC and survived into the pores. In
418 conclusion, WSOCs influence the suitability of BC for environmental applications. Previous
419 studies proposed that high amounts of PAHs[49], phenolic and carboxylic acids[4,8] in BC WSOCs
420 caused harmful effects on cress seeds. In this study, fulvic-like WSOCs and concentrations of
421 VFA< 3mg/g induced statistically significant positive effects on the seedlings of cress,
422 corroborating the hypothesis that the complex biological effects of BC WSOCs are the results of
423 an interaction between contrasting factors.[3,40] However, this study demonstrated that BC to soil
424 application can be sustainable when BC contamination (organic and inorganic) is limited.

425 **REFERENCES**

426 (1) Lehmann, J.; Gaunt, J.; Rondon, M. Bio-char sequestration in terrestrial ecosystems - A
427 review. *Mitig. Adapt. Strateg. Glob. Chang.* **2006**, *11* (2), 403–427.

428 (2) Bachmann, H. J.; Bucheli, T. D.; Dieguez-Alonso, A.; Fabbri, D.; Knicker, H.; Schmidt, H.

P.; Ulbricht, A.; Becker, R.; Buscaroli, A.; Buerge, D.; et al. Toward the Standardization of Biochar Analysis: The COST Action TD1107 Interlaboratory Comparison. *J. Agric. Food Chem.* **2016**, *64* (2), 513–527.

(3) Lou, Y.; Joseph, S.; Li, L.; Graber, E. R.; Liu, X.; Pan, G. Water extract from straw biochar used for plant growth promotion: An initial test. *BioResources* **2016**, *11* (1), 249–266.

(4) Rombolà, A. G.; Marisi, G.; Torri, C.; Fabbri, D.; Buscaroli, A.; Ghidotti, M.; Hornung, A. Relationships between Chemical Characteristics and Phytotoxicity of Biochar from Poultry Litter Pyrolysis. *J. Agric. Food Chem.* **2015**, *63* (30), 6660–6667.

(5) Buss, W.; Mašek, O. Mobile organic compounds in biochar - A potential source of contamination - Phytotoxic effects on cress seed (Lepidium sativum) germination. *J. Environ. Manage.* **2014**, *137*, 111–119.

(6) Sun, D.; Meng, J.; Liang, H.; Yang, E.; Huang, Y.; Chen, W.; Jiang, L.; Lan, Y.; Zhang, W.; Gao, J. Effect of volatile organic compounds absorbed to fresh biochar on survival of Bacillus mucilaginosus and structure of soil microbial communities. *J. Soils Sediments* **2014**, *15* (2), 271–281.

(7) Smith, C. R.; Buzan, E. M.; Lee, J. W. Potential impact of biochar water-extractable substances on environmental sustainability. *ACS Sustain. Chem. Eng.* **2013**, *1* (1), 118–126.

(8) Smith, C. R.; Hatcher, P. G.; Kumar, S.; Lee, J. W. Investigation into the Sources of Biochar Water-Soluble Organic Compounds and Their Potential Toxicity on Aquatic Microorganisms. *ACS Sustain. Chem. Eng.* **2016**, *4* (5), 2550–2558.

(9) Riedel, T.; Iden, S.; Geilich, J.; Wiedner, K.; Durner, W.; Biester, H. Changes in the molecular composition of organic matter leached from an agricultural topsoil following addition of biomass-derived black carbon (biochar). *Org. Geochem.* **2014**, *69*, 52–60.

(10) Uchimiya, M.; Liu, Z.; Sistani, K. Field-scale fluorescence fingerprinting of biochar-borne dissolved organic carbon. *J. Environ. Manage.* **2016**, *169*, 184–190.

(11) Ghidotti, M.; Fabbri, D.; Hornung, A. Profiles of Volatile Organic Compounds in Biochar: Insights into Process Conditions and Quality Assessment. *ACS Sustain. Chem. Eng.* **2017**, *5* (1), 510-517

(12) Buss, W.; Graham, M. C.; MacKinnon, G.; Mašek, O. Strategies for producing biochars with minimum PAH contamination. *J. Anal. Appl. Pyrolysis* **2016**, *119*, 24–30.

(13) Madej, J.; Hilber, I.; Bucheli, T. D.; Oleszczuk, P. Biochars with low polycyclic aromatic hydrocarbon concentrations achievable by pyrolysis under high carrier gas flows irrespective of oxygen content or feedstock. *J. Anal. Appl. Pyrolysis* **2016**, *122*, 365–369.

(14) Lin, Y.; Munroe, P.; Joseph, S.; Henderson, R.; Ziolkowski, A. Water extractable organic carbon in untreated and chemical treated biochars. *Chemosphere* **2012**, *87* (2), 151–157.

(15) Cerqueira, W. V; Rittl, T. F.; Novotny, E. H.; Pereira Netto, A. D. High throughput pyrogenic carbon (biochar) characterisation and quantification by liquid chromatography. *Anal. Methods* **2015**, *7* (19), 8190–8196.

(16) Smith, C. R.; Sleighter, R. L.; Hatcher, P. G.; Lee, J. W. Molecular characterization of inhibiting biochar water-extractable substances using electrospray ionization fourier transform ion cyclotron resonance mass spectrometry. *Environ. Sci. Technol.* **2013**, *47* (23), 13294–13302.

(17) Uchimiya, M.; Hiradate, S.; Antal, M. J. Influence of carbonization methods on the aromaticity of pyrogenic dissolved organic carbon. *Energy and Fuels* **2015**, *29* (4), 2503–2513.

(18) Jamieson, T.; Sager, E.; Guéguen, C. Characterization of biochar-derived dissolved organic

matter using UV-visible absorption and excitation-emission fluorescence spectroscopies. *Chemosphere* **2014**, *103*, 197–204.

(19) Uchimiya, M.; Ohno, T.; He, Z. Pyrolysis temperature-dependent release of dissolved organic carbon from plant, manure, and biorefinery wastes. *J. Anal. Appl. Pyrolysis* **2013**, *104*, 84–94.

(20) Samorì, C.; López Barreiro, D.; Vet, R.; Pezzolesi, L.; Brilman, D. W. F.; Galletti, P.; Tagliavini, E. Effective lipid extraction from algae cultures using switchable solvents. *Green Chem.* **2013**, *15* (2), 353–356.

(21) Montalti, M.; Credi, A.; Prodi, L.; Gandolfi, M.T.; Handbook of photochemistry.; CRC press, 2006, 561-581

(22) Andersson, C. A.; Bro, R. The N-way Toolbox for MATLAB. *Chemom. Intell. Lab. Syst.* **2000**, *52* (1), 1–4.

(23) Murphy, K. R.; Stedmon, C. A.; Graeber, D.; Bro, R. Fluorescence spectroscopy and multi-way techniques. PARAFAC. *Anal. Methods* **2013**, *5* (23), 6557.

(24) Stedmon, C. A.; Bro, R. Characterizing dissolved organic matter fluorescence with parallel factor analysis: a tutorial. *Limnol. Oceanogr. Methods* **2008**, *6* (11), 572–579.

(25) Jiménez, J. J.; Bernal, J. L.; Nozal, M. J.; Toribio, L.; Bernal, J. Profile and relative concentrations of fatty acids in corn and soybean seeds from transgenic and isogenic crops. *J. Chromatogr. A* **2009**, *1216* (43), 7288–7295.

(26) Sleighter, R. L.; Hatcher, P. G. The application of electrospray ionization coupled to ultrahigh resolution mass spectrometry for the molecular characterization of natural organic matter. *Journal of Mass Spectrometry*. May 2007, pp 559–574.

(27) Stankovikj, F.; McDonald, A. G.; Helms, G. L.; Garcia-Perez, M. Quantification of Bio-Oil

functional Groups and Evidences of the Presence of Pyrolytic Humins. *Energy and Fuels* **2016**, *30* (8), 6505–6524.

(28) Kim, S.; Kramer, R. W.; Hatcher, P. G. Graphical Method for Analysis of Ultrahigh-Resolution Braodband mass spectra of Natural Organic Matter, the Van Krevelen diagram. *Anal. Chem.* **2003**, *75* (20), 5336–5344.

(29) Ohno, T.; He, Z.; Sleighter, R. L.; Honeycutt, C. W.; Hatcher, P. G. Ultrahigh Resolution Mass Spectrometry and Indicator Species Analysis to Identify Marker Components of Soil- and Plant Biomass-Derived Organic Matter Fractions. *Environ. Sci. Technol.* **2010**, *44* (22), 8594–8600.

(30) Hockaday, W. C.; Purcell, J. M.; Marshall, A. G.; Baldock, J. a; Hatcher, P. G. Electrospray and photoionization mass spectrometry for the characterization of organic matter in natural waters : a qualitative assessment. *Limnol. Oceanogr. Methods* **2009**, *7*, 81–95.

(31) Opsahl, S.; Benner, R. Photochemical reactivity of dissolved lignin in river and ocean waters. *Limnol. Oceanogr.* **1998**, *43* (6), 1297–1304.

(32) Hertzog, J.; Carré, V.; Le Brech, Y.; Dufour, A.; Aubriet, F. Toward Controlled Ionization Conditions for ESI-FT-ICR-MS Analysis of Bio-Oils from Lignocellulosic Material. *Energy and Fuels* **2016**, *30* (7), 5729–5739.

(33) Andrilli, J. D.; Foreman, C. M.; Marshall, A. G.; Mcknight, D. M. Organic Geochemistry Characterization of IHSS Pony Lake fulvic acid dissolved organic matter by electrospray ionization Fourier transform ion cyclotron resonance mass spectrometry and fluorescence spectroscopy. *Org. Geochem.* **2013**, *65*, 19–28.

(34) He, Z.; Ohno, T.; Wu, F.; Olk, D. C.; Honeycutt, C. W.; Olanya, M. Capillary Electrophoresis and Fluorescence Excitation-Emission Matrix Spectroscopy for

521 Characterization of Humic Substances. *Soil Sci. Soc. Am. J.* **2008**, *72* (5), 1248.
522 (35) Mobed, J. J.; Hemmingsen, S. L.; Autry, J. L.; Mcgown, L. B. Fluorescence characterization
523 of IHSS humic substances: Total luminescence spectra with absorbance correction.
524 *Environ. Sci. Technol.* **1996**, *30* (10), 3061–3065.
525 (36) Ferretto, N.; Tedetti, M.; Guigue, C.; Mounier, S.; Redon, R.; Goutx, M. Identification and
526 quantification of known polycyclic aromatic hydrocarbons and pesticides in complex
527 mixtures using fluorescence excitation-emission matrices and parallel factor analysis.
528 *Chemosphere* **2014**, *107*, 344–353.
529 (37) van Zwieten, L.; Kimber, S.; Morris, S.; Chan, K. Y.; Downie, A.; Rust, J.; Joseph, S.;
530 Cowie, A. Effects of biochar from slow pyrolysis of papermill waste on agronomic
531 performance and soil fertility. *Plant Soil* **2010**, *327* (1), 235–246.
532 (38) Buss, W.; Graham, M. C.; Shepherd, J. G.; Mašek, O. Risks and benefits of marginal
533 biomass-derived biochars for plant growth. *Sci. Total Environ.* **2016**, *569–570*, 496–506.
534 (39) Flematti, G. R. A Compound from Smoke That Promotes Seed Germination. *Science (80-.*
535 *).* **2004**, *305* (5686), 977–977.
536 (40) Kochanek, J.; Long, R. L.; Lisle, A. T.; Flematti, G. R. Karrikins Identified in Biochars
537 Indicate Post-Fire Chemical Cues Can Influence Community Diversity and Plant
538 Development. *PLoS One* **2016**, *11* (8), e0161234.
539 (41) Calvo, P.; Nelson, L.; Kloepper, J. W. Agricultural uses of plant biostimulants. *Plant Soil*
540 **2014**, *383* (1–2), 3–41.
541 (42) Amendola, C.; Montagnoli, A.; Terzaghi, M.; Trupiano, D.; Oliva, F.; Baronti, S.; Miglietta,
542 F.; Chiatante, D.; Scippa, G. S. Short-term effects of biochar on grapevine fine root
543 dynamics and arbuscular mycorrhizae production. *Agric. Ecosyst. Environ.* **2017**, *239*, 236–

245.

(43) Sun, J.; Drosos, M.; Mazzei, P.; Savy, D.; Todisco, D.; Vinci, G.; Pan, G.; Piccolo, A. The molecular properties of biochar carbon released in dilute acidic solution and its effects on maize seed germination. *Sci. Total Environ.* **2017**, *576*, 858–867.

(44) Xiao, F.; Pignatello, J. J. π+-π Interactions between (hetero)aromatic amine cations and the graphitic surfaces of pyrogenic carbonaceous materials. *Environ. Sci. Technol.* **2015**, *49* (2), 906–914.

(45) Ahmad, M.; Rajapaksha, A. U.; Lim, J. E.; Zhang, M.; Bolan, N.; Mohan, D.; Vithanage, M.; Lee, S. S.; Ok, Y. S. Biochar as a sorbent for contaminant management in soil and water: A review. *Chemosphere*. 2014, pp 19–23.

(46) Taherymoosavi, S.; Joseph, S.; Munroe, P. Characterization of organic compounds in a mixed feedstock biochar generated from Australian agricultural residues. *J. Anal. Appl. Pyrolysis* **2015**, *120*, 441–449.

(47) Stenson, A. C.; Landing, W. M.; Marshall, A. G.; Cooper, W. T. Ionization and fragmentation of humic substances in Electrospray Ionization Fourier Transform-Ion Cyclotron Resonance Mass Spectrometry. *Anal. Chem.* **2002**, *74* (17), 4397–4409.

(48) Qu, X.; Fu, H.; Mao, J.; Ran, Y.; Zhang, D.; Zhu, D. Chemical and structural properties of dissolved black carbon released from biochars. *Carbon N. Y.* **2016**, *96*, 759–767.

(49) Rogovska, N.; Laird, D.; Cruse, R. M.; Trabue, S.; Heaton, E. Germination Tests for Assessing Biochar Quality. *J. Environ. Qual.* **2012**, *41* (4), 1014.

TOC

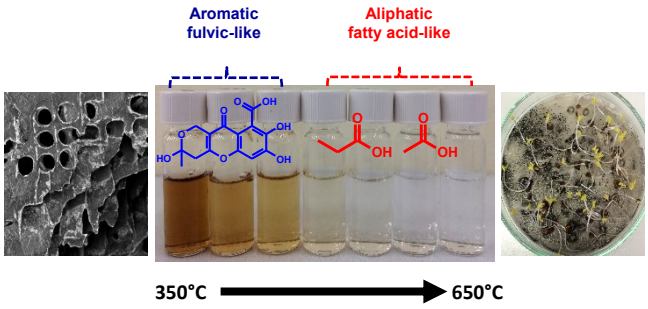

FIGURES

Figure 1: Total ion chromatograms of BC350 and OL350 WSOCs after DI-SPME-GC-MS analysis. Principal compounds are evidenced, while the complete lists of the volatile and semi-volatile WSOCs are reported in Tables S1 and S2

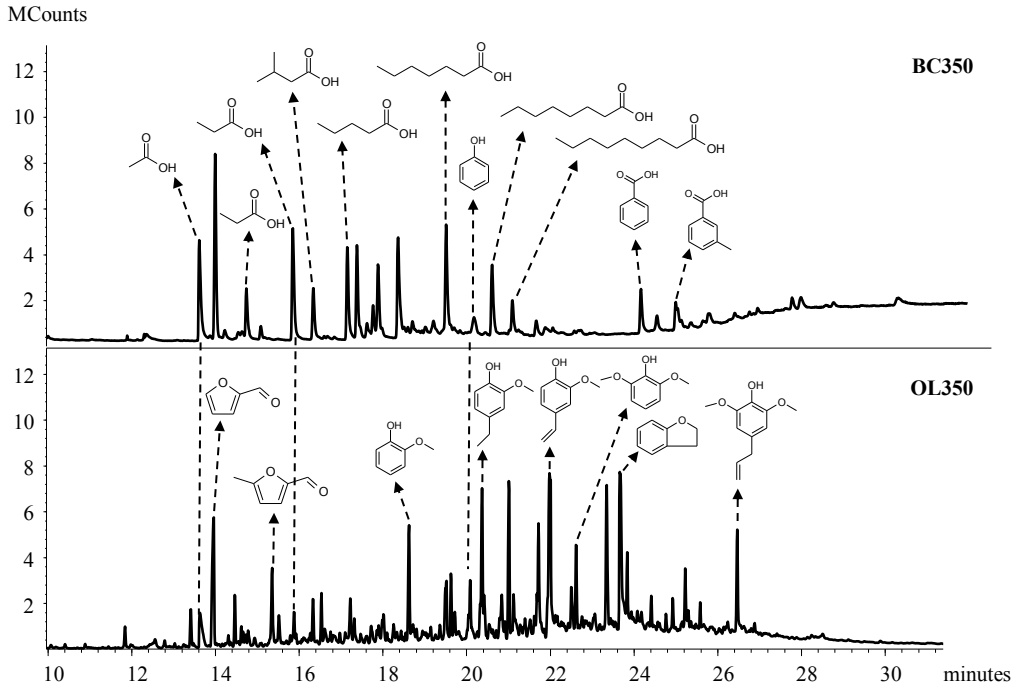

Figure 2: Van Krevelen diagrams of WSOCs by ESI(-)FT-ICR-MS, in BC produced at 350, 450, 650 °C and the corresponding OL

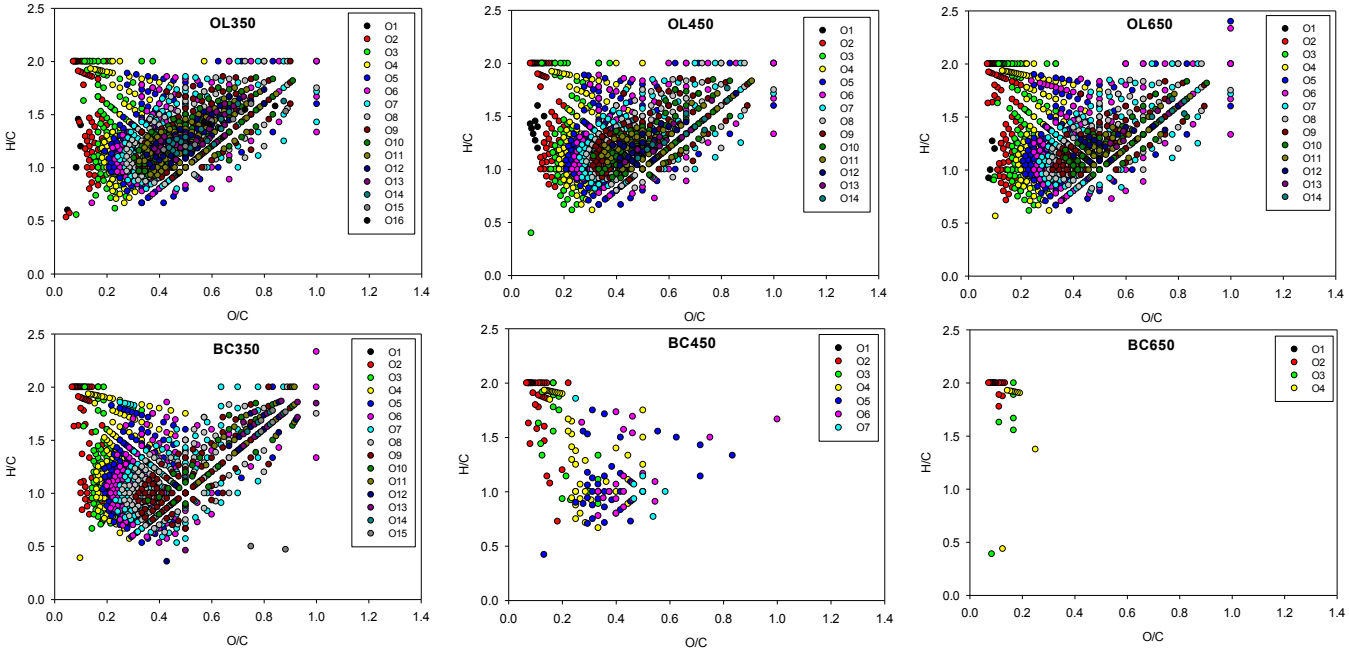

Figure 3: Plots of DBE vs Carbon number of BC 350, 450, 650 WSOCs and the corresponding OL

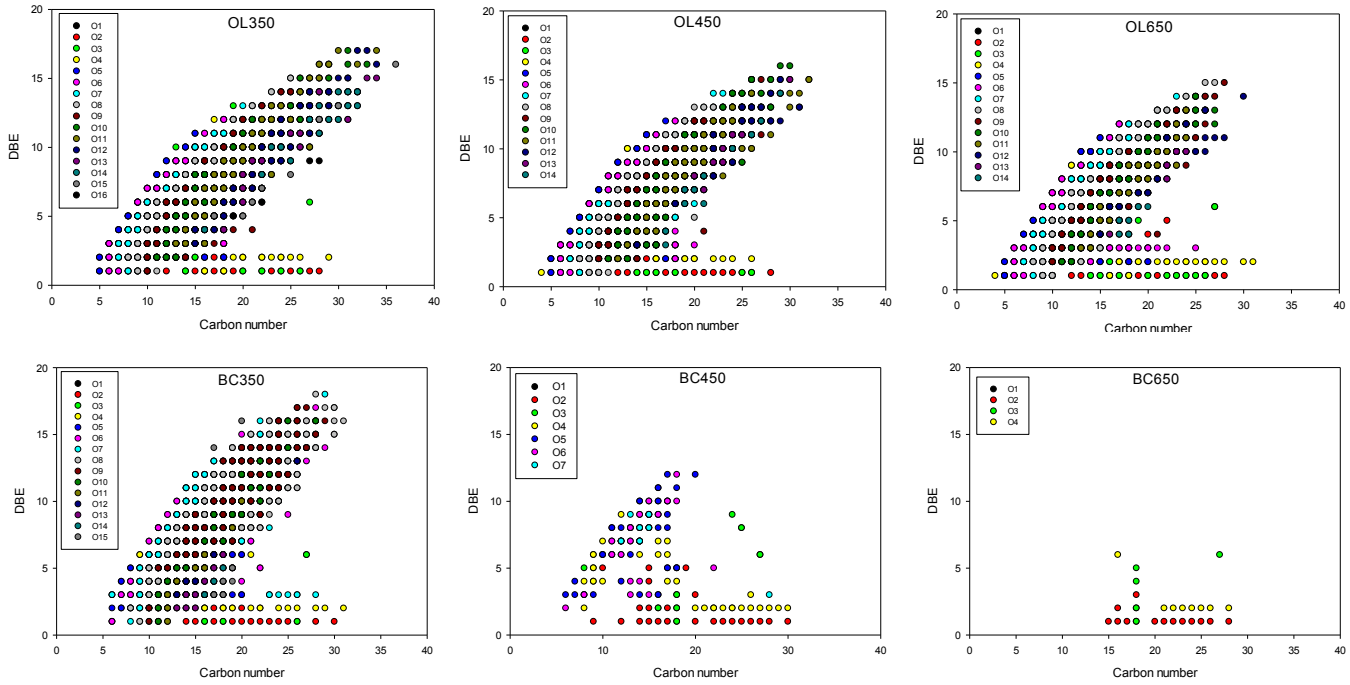

Figure 4: Spectral characteristics of the four components (C1-4) PARAFAC modeling of BC and OL WSOCs

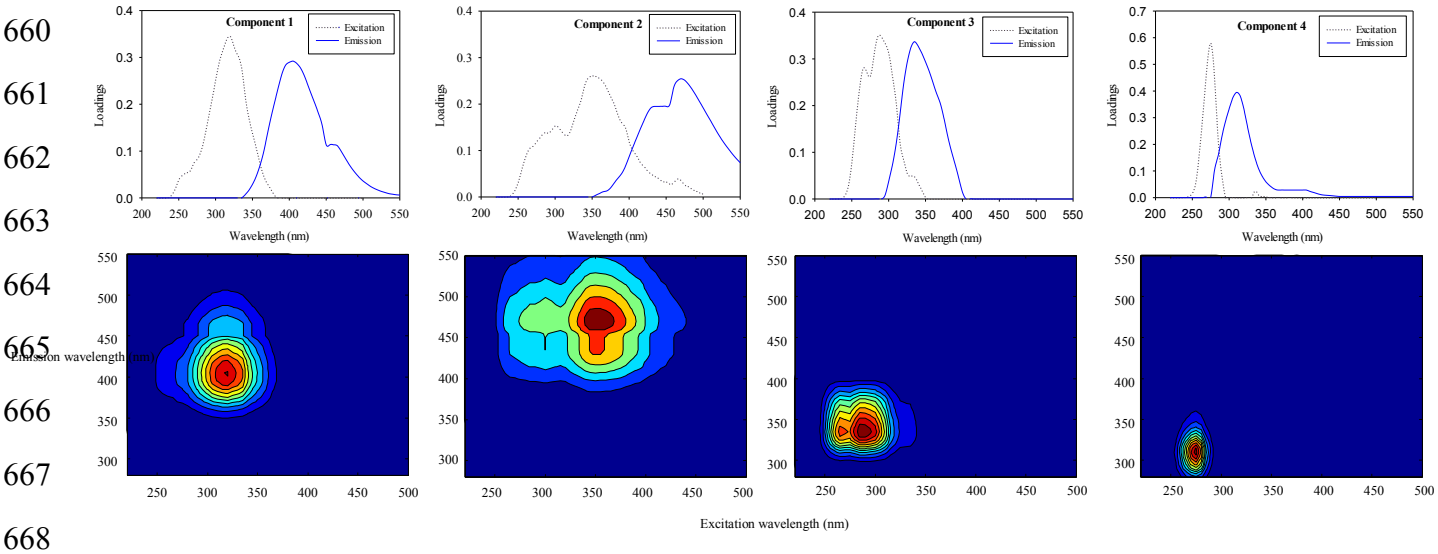

Figure 5: Box and whisker plots of shoot and root lengths (cm) of the cress seedlings for each treatment with (BC), without BC (Control) and VFA solution. 25-75 percent quartiles are drawn using a box. The median is shown with a horizontal line inside the box. Horizontal lines outside the box represents the variability outside the lower and upper quartiles. Values >1.5 times the box height are reported as circles.

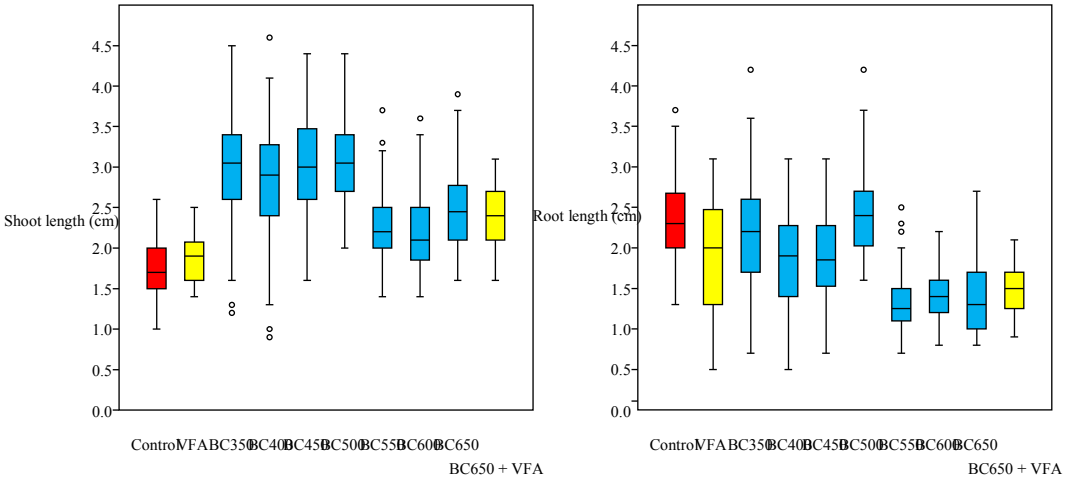

ACKNOWLEDGEMENTS

Part of the study was performed within the collaboration agreement between the University of Bologna and Fraunhofer Institute for Environmental, Safety and Energy Technology (UMSICHT), Germany. The authors would like to thank Jeannette Manzi (Department of Chemistry "Giacomo Ciamician", University of Bologna) for the technical assistance during fluorescence spectroscopy analysis.

CORRESPONDING AUTHOR

*Michele Ghidotti, Interdepartmental Centre for Industrial Research "Energy and Environment" and Department of Chemistry "Giacomo Ciamician", University of Bologna, via S. Alberto 163, I-48123 Ravenna, Italy; michele.ghidotti2@unibo.it, +39 0544 937388

SUPPORTING INFORMATION

Figures and Tables with detailed quantitative, semi-quantitative and qualitative results of the analysis of BC and OL WSOCs by DI-SPME-GC-MS, ESI-FT-ICR-MS and Fluorescence-PARAFAC.